



PCCP

Gas phase protonated nicotine is a mixture of pyridine- and pyrrolidine-protonated conformers: implications for its native structure in the nicotinic acetyl-choline receptor

Journal:	<i>Physical Chemistry Chemical Physics</i>
Manuscript ID	CP-ART-11-2021-005175
Article Type:	Paper
Date Submitted by the Author:	12-Nov-2021
Complete List of Authors:	Takeda, Naoya; Tokyo Institute of Technology Hirata, Keisuke; Tokyo Institute of Technology Tsuruta, Kazuya; Tokyo Institute of Technology Santis, Garrett D.; University of Washington Sotiris, XS; Pacific Northwest National Laboratory Ishiuchi, Shun-ichi; Tokyo Institute of Technology Fujii, Masaaki; Tokyo Institute of Technology

SCHOLARONE™
Manuscripts

Gas phase protonated nicotine is a mixture of pyridine- and pyrrolidine-protonated conformers: implications for its native structure in the nicotinic acetylcholine receptor

Naoya Takeda,^{1,2,‡} Keisuke Hirata,^{1,3,4,‡} Kazuya Tsuruta,^{1,2} Garrett D. Santis,⁵ Sotiris S. Xantheas,^{4,5,6,*} Shun-ichi Ishiuchi,^{1,3,4,*} and Masaaki Fujii^{1,2,4,*}

¹ Laboratory for Chemistry and Life Science, Institute of Innovative Research, Tokyo Institute of Technology, 4259 Nagatsuta-cho, Midori-ku, Yokohama, 226-8503, Japan

² School of Life Science and Technology, Tokyo Institute of Technology, 4259 Nagatsuta-cho, Midori-ku, Yokohama, Kanagawa, 226-8503, Japan

³ Department of Chemistry, School of Science, Tokyo Institute of Technology, 2-12-1 4259 Ookayama, Meguro-ku, Tokyo, 152-8550, Japan

⁴ Tokyo Tech World Research Hub Initiative (WRHI), Institute of Innovation Research, Tokyo Institute of Technology, 4259, Nagatsuta-cho, Midori-ku, Yokohama, 226-8503, Japan

⁵ Department of Chemistry, University of Washington, Seattle, WA 98195, United States

⁶ Advanced Computing, Mathematics and Data Division, Pacific Northwest National Laboratory, 902 Battelle Boulevard, P.O. Box 999, MS K1-83, Richland, WA 99352, United States

‡ Contributed equally.

Nicotine, infrared spectroscopy, electronic structure, protomers

ABSTRACT: The infrared (IR) spectra of gas phase protonated nicotine has been measured in the never-before probed N-H “fingerprint region” (3,200–3,500 cm^{-1}). The protonated molecules generated by an electrospray source are thermalized in the first ion trap with water vapor and He gas at a pre-determined temperature prior to being probed by IR spectroscopy in the second ion trap at 4 K. The IR spectra exhibit two N-H stretching bands which are assigned to the pyridine and pyrrolidine protomers with the aid of high-level electronic structure calculations. This finding is in sharp contrast to previous spectroscopic studies that suggested a single population of the pyridine protomer. The relative populations of the two protomers vary by changing the temperature of the thermalizing trap from 180 K – 300 K. The relative conformer populations at 240 K and 300 K are well reproduced by the theoretical calculations, unequivocally determining that gas phase nicotine is a 3:2 mixture of both pyridine and pyrrolidine protomers at room temperature. The thermalizing anhydrous vapor does not result in any population change. It rather demonstrates the catalytic role of water in achieving equilibrium between the two protomers. The combination of IR spectroscopy and electronic structure calculations establish the small energy difference between the pyridine and pyrrolidine protomers in nicotine. One of the gas phase nicotine pyrrolidine protomers has the closest conformational resemblance among all low-lying energy isomers with the X-ray structure of nicotine in the nicotinic acetylcholine receptor (nAChR). The important role of a single water molecule that is present in the binding protein is suggested.

1. Introduction

Nicotine (NIC) is a heteroaromatic molecule consisting of pyridine and pyrrolidine rings (Figure 1 top). It is the major alkaloid in tobacco and causes serious health problems through addiction.¹⁻³ It imitates the function of a natural neurotransmitter, acetylcholine, and binds as an agonist to the nicotinic acetylcholine receptor (nAChR) in the human brain. Because neural ion signaling is mediated by the activation of these ligand-gated nAChRs, they are regarded as one of the most promising drug targets.⁴ Single-crystal X-ray diffraction (SC-XRD) has provided insight into the structural mechanism for this process.⁵⁻⁹ The binding mode of protonated nicotine (NIC-H⁺) to the nAChR was first deduced by an acetylcholine-binding protein (AChBP), which shows a sequence similarity to the α subunits of nAChR.⁶ Subsequently, the $\alpha_4\beta_2$ -type nAChR was crystalized and the nicotine binding was shown.^{8,9} The SC-XRD analysis indicates that the pyrrolidine nitrogen of NIC interacts with the carbonyl oxygen of tryptophane (Trp) in the nAChR. In addition, the pyridine nitrogen of NIC forms a hydrogen bond to leucine and methionine mediated by a single water molecule that is present in the binding protein (AChBP). Despite several previous studies, the molecular-level mechanism controlling the function of NIC as an agonist is still unclear. NIC is expected to be protonated under physiological conditions,^{10,11} yet the protonation sites cannot be obtained from SC-XRD studies since the method is insensitive to protons. The protonation site directly affects the binding in nAChRs, thus the structure and relative population of the NIC protomers are indispensable in understanding the binding mechanism of NIC in nAChR.

Previous structural investigations using ultraviolet (UV) and infrared (IR) spectroscopies have been intensively focused on NIC-H⁺, which is the prevailing species at physiological condition.¹⁰ NIC has two possible protonation sites on the nitrogen atom either on the pyridine (Pyri-NIC-H⁺) or the pyrrolidine (Pyrro-NIC-H⁺) rings, resulting in the two protomers shown in Figure 1 (top). The NIC-H⁺ protomer has been investigated in both the gas phase¹¹⁻¹⁴ and in solution.^{10,11} UV absorption spectroscopy has determined two pK_a values of nicotine in water at $T = 298$ K (pK_a = 2.85 for the pyridine ring, 7.89 for the pyrrolidine ring),^{10,11} indicating that nicotine is in the form of the Pyrro-NIC-H⁺ in aqueous solution at physiological pH (~7.4),^{10,11} a fact subsequently supported by IR spectroscopy.¹² In contrast, the protonation site of NIC-H⁺ in the gas phase has not been conclusively determined. In an earlier study, the gas-phase acidity of nicotine was measured by Fourier-transform ion cyclotron resonance mass spectrometry (FT-ICR-MS).¹¹ The results indicated that both the Pyri-NIC-H⁺ and Pyrro-NIC-H⁺ protomers coexist in the gas phase. However, a subsequent study using IR multiphoton photodissociation spectroscopy in the mid-IR range suggested that only the Pyri-NIC-H⁺ protomer was observed in the gas phase.¹² Previous *ab initio* calculations of NIC-H⁺ performed at the MP2/aug-cc-pVTZ level of theory indicated that the two protomers are energetically equivalent, advocating their coexistence in the gas phase.¹⁵ Ion mobility mass spectrometry combined with photofragment detection found the coexistence of two species, of which the parent ions were estimated to be Pyri-NIC-H⁺ and Pyrro-NIC-H⁺.¹³ The observed fragment ions were $m/z = 84$ (loss of neutral pyridine) for the presence of Pyri-NIC-H⁺ and $m/z = 132$ (loss of NH₂CH₃) for the presence of Pyrro-NIC-H⁺. Although the dissociation pathways were estimated, the observation of both fragment ions does not constitute direct evidence of the existence of Pyri- and Pyrro-NIC-H⁺. Furthermore, all previous gas phase experiments are plagued with the problem of kinetic trapping originating from the electrospray ionization (ESI) source that generates the protonated species. It is a well-known problem of ESI sources that the dominant species in solution (in this case Pyrro-NIC-H⁺) remains in gas phase even if the species is less stable in gas phase. This kinetic trapping is caused by the slow / soft evaporation of solvent molecules during the ESI process, and thus the observed species do not always reflect the gas phase equilibrium. Therefore, both the protonation sites and the relative populations of gas phase NIC-H⁺ are still unresolved due to the contentious issue of kinetic trapping. These gas-phase populations are highly significant when considering the anhydrous environment in the human brain receptor.^{16,17}

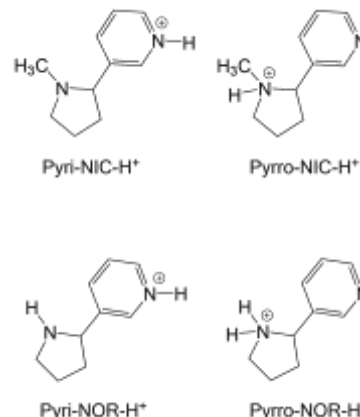


Figure 1. Protomers of nicotine (NIC-H⁺, top) and normicotine (NOR-H⁺, bottom).

Similar to NIC, protomers of nornicotine (NOR) have previously attracted interest. NOR is a metabolite of nicotine produced by N-demethylation (see Figure 1 bottom). Its potential bioactivity is important because of its abundance and long lifetime in the brain.¹⁸⁻²⁰ In general, NOR shows lower affinity to the $\alpha_4\beta_2$ -type nAChR than NIC but a comparably high affinity to other receptors such as the α_7 -type nAChR.²¹ NOR is protonated on the pyrrolidine nitrogen (Pyrro-NOR-H⁺) in water at physiological pH, similar to NIC.²² However, the gas-phase acidity of NOR, determined by FT-ICR, suggests that NOR-H⁺ has only a pyridine-protomer (Pyri-NOR-H⁺) in the gas phase.¹¹ No IR/UV spectroscopic study has been reported to date for gas-phase NOR-H⁺, and therefore its protonation site in the gas phase has not unambiguously been determined yet.

In this study we investigated the protonation sites of NIC-H⁺ and NOR-H⁺ in the gas phase by means of experimental cryogenic ion trap IR spectroscopy and theoretical electronic structure methods. We measured the IR spectra in the never-before probed 3 μm region (3200–3500 cm^{-1}), corresponding to the “fingerprint” region of the pyridine/pyrrolidine N-H stretches. The population of pyridine- and pyrrolidine-protomers in the gas phase was determined using the experimentally observed and theoretically predicted IR absorption band intensities. The advantage of our experimental design is the use of double ion traps,²³ which circumvents the problem of kinetic trapping.²⁴ The protonated molecules generated by the ESI source are first introduced into the thermalizing ion trap and kept for a long period of time (~ 50 ms) at a well-defined temperature (such as 300K) together with the buffer gas. The trapped species are well thermalized in the first ion trap so that thermal equilibrium of the protomers is achieved. The thermalized sample molecules are subsequently introduced into the ultracold quadrupole ion trap (QIT) and probed by spectroscopy while their population is frozen through rapid cooling by He gas at $T = 4\text{K}$. The rapid freezing process produces sharp spectra so the various species and their population can be assigned clearly. The advantage of the double ion trap setup to solve the kinetic trapping is well demonstrated in the recent spectroscopic work on metal ion – peptide complexes.²⁴ Here, we will rely on this setup to provide the unambiguous assignment of NIC-H⁺ and NOR-H⁺ in gas phase at physiological temperature ($T = 300\text{K}$).

2. Methods

The experiments were carried out using a cryogenic ion trap apparatus combined with an electrospray ion source (Figure S1 in Supporting Information).²⁵⁻³⁰ Details of the experimental setup were described elsewhere.^{31, 32} Enantiomerically pure (–)-nicotine (FUJIFILM Wako) and racemic (\pm)-nornicotine (FUJIFILM Wako) were used because only (–)-nicotine is present in the *Nicotiana* plant, while both (+)- and (–)-nornicotine exist in nature.^{33, 34} NIC or NOR were dissolved in acidified methanol (1 μM) with 0.5 % formic acid. This solution was electrosprayed to form fine droplets containing the protonated species (NIC-H⁺/NOR-H⁺). The solvents in the droplets were completely desolvated in a glass capillary heated at 60 °C. The desolvated ions were efficiently collected by an ion funnel. NIC-H⁺ (or NOR-H⁺) were mass-selected by a Q-MS1 and guided into an octupole linear ion trap (thermalizing trap) kept at selected temperatures ranging from $T = 180 - 300\text{K}$. Here, the ions were trapped for 50 ms, colliding with He or mixture of He/H₂O vapor. The ions were mass-filtered by a second quadrupole mass spectrometer (Q-MS2) to ensure that only NIC-H⁺ (NOR-H⁺) were then passed to a quadrupole bender and introduced into a quadrupole ion trap (QIT), which was kept at $T = 4\text{K}$ by a closed-cycle He refrigerator. H₂ (20%)/He buffer gas was injected into the QIT by a pulsed valve. The collisions with the buffer gas cooled the ions down to $\sim 10\text{K}$, enabling H₂ molecules to attach to the ions. The trapped cluster ions were then irradiated with a tunable IR laser (LaserVision, OPO/OPA). When the IR laser is tuned to a vibrational resonance, the energy from the absorbed photon detaches the H₂ molecules to yield the bare NIC-

H⁺ (NOR-H⁺) as a fragment, which is then detected by a time-of-flight mass spectrometer (TOF-MS). Thus, IR photodissociation (IRPD) spectra, which correspond to the IR absorption spectra, can be measured by monitoring the intensity of the bare ions as a function of the IR wavenumber.

The energies of NIC and NOR were calculated to investigate the thermodynamics between the protomers. The lowest energy structures were taken from Yoshida et. al.¹⁵ The MP2/Complete Basis Set (CBS) limit for the electronic energy difference between conformers was estimated using the 4-5 extrapolation³⁵⁻³⁷ with the aug-cc-pVnZ, $n = D, T, Q$ basis sets³⁸ using NWChem.³⁹ Harmonic and thermal corrections were calculated at the ω B97-XD/aug-cc-pVDZ level of theory for $T = 180, 240,$ and 300 K to compare with experiment. The percentages of each protomer were calculated from the Boltzmann populations of NIC and NOR following

$$P_i = e^{-\Delta G_i/RT} \quad (1)$$

and normalized to the total population. Theoretical IR spectra were calculated at the ω B97XD/aug-cc-pVTZ (scaling factor: 0.941⁴⁰) level of theory using the most stable conformations reported previously (Cartesian coordinates in S2-S6 in SI).¹⁵

3. Results and Discussion

Figure 2c shows the experimental IRPD spectrum of NIC-H⁺ in the 3200–3500 cm⁻¹ spectral range without the thermalizing trap. The bands at 3254 and 3394 cm⁻¹ are assigned to the N-H stretching vibrations. Because NIC-H⁺ has only a single N-H bond, the appearance of two N-H stretching bands indicates that the two protomers (Pyri-NIC-H⁺ and Pyrro-NIC-H⁺) coexist in the gas phase. Our previous calculations¹⁵ support the existence of a single Pyri-NIC-H⁺ (*S, trans, anti*) protomer and two almost isoenergetic Pyrro-NIC-H⁺ (*N, trans, anti*) and (*N, trans, syn*) protomers that are indistinguishable from each other in the IR (we simply refer to them as Pyrro-NIC-H⁺ hereafter). To confirm the coexistence of the Pyri- and Pyrro-protomers, the observed spectra were compared to the theoretical IR spectra of Pyri- and Pyrro-NIC-H⁺ shown in Figure 2a and 2b, respectively. The theoretical IR spectrum of Pyri-NIC-H⁺ is associated with the strong band of the pyridine N-H stretch at 3392 cm⁻¹ (IR intensity: 148 km mol⁻¹), which reproduces the observed strong transition at 3394 cm⁻¹. The theoretical spectrum of Pyrro-NIC-H⁺ shows a relatively weaker band at 3273 cm⁻¹ (29 km mol⁻¹) ascribed to the pyrrolidine N-H stretch, which reasonably matches the experimentally observed weaker N-H stretch band at 3254 cm⁻¹. A tiny band at 3280 cm⁻¹ may be derived from another pyrrolidine protomer such as the less stable *cis* conformer.¹⁵ However, the fact that these conformers are higher up in energy (> 3 kcal/mol from the Pyri-NIC-H⁺ minimum) and thus probably not accessible at this temperature, this band maybe also due to an overtone or combination band.

Although the IRPD spectrum in the N-H stretching vibrational range clearly shows the spectral signature of both Pyri-NIC-H⁺ and Pyrro-NIC-H⁺, we cannot exclude the possibility that Pyrro-NIC-H⁺ remains in the gas phase because of kinetic trapping. To reach a definite conclusion, we measured the IRPD spectra of NIC-H⁺ after the thermalizing trap, shown in Figure 2d-2f, at various temperatures of the thermalizing trap that are indicated in the figure. Here, the thermalizing trap is filled with only He buffer

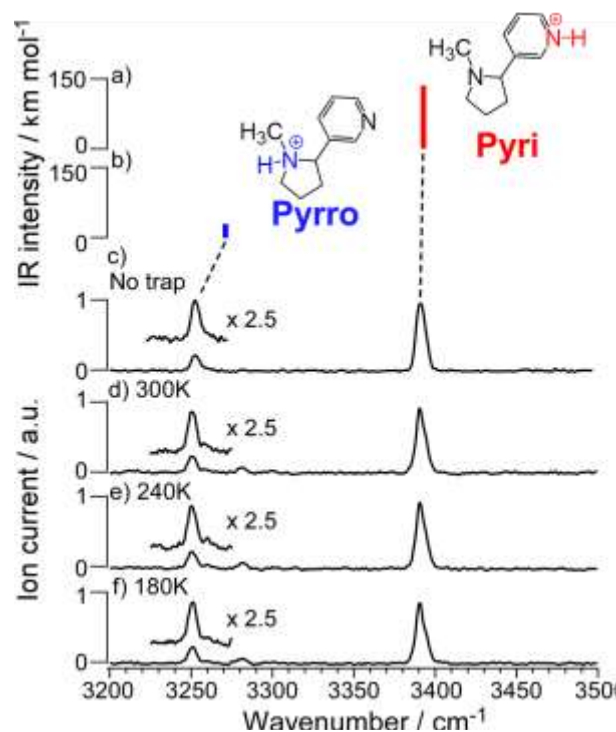


Figure 2. Theoretical IR spectra of (a) Pyri-NIC-H⁺ and (b) Pyrro-NIC-H⁺ in the 3200–3500 cm⁻¹ spectral range. The theoretical spectra were calculated at the ω B97XD/aug-cc-pVTZ level (scaling factor: 0.941). Experimental IRPD spectra of NIC-H⁺ (c) without thermalizing trap, and with thermalizing trap at (d) $T=300$ K, (e) $T=240$ K and (f) $T=180$ K of He buffer gas only. No change in the relative intensity between Pyrro- and Pyri-NIC-H⁺ was observed.

gas. As can be seen in the figure, almost no change is found in the IRPD spectra even though the temperatures are varied from 180 – 300 K. This lack of change in the spectra is indicative of kinetic trapping.

To enhance the proton exchange among protomers, we introduced water vapor together with He buffer gas into the thermalizing trap and repeated the same measurements. He gas is an efficient temper-

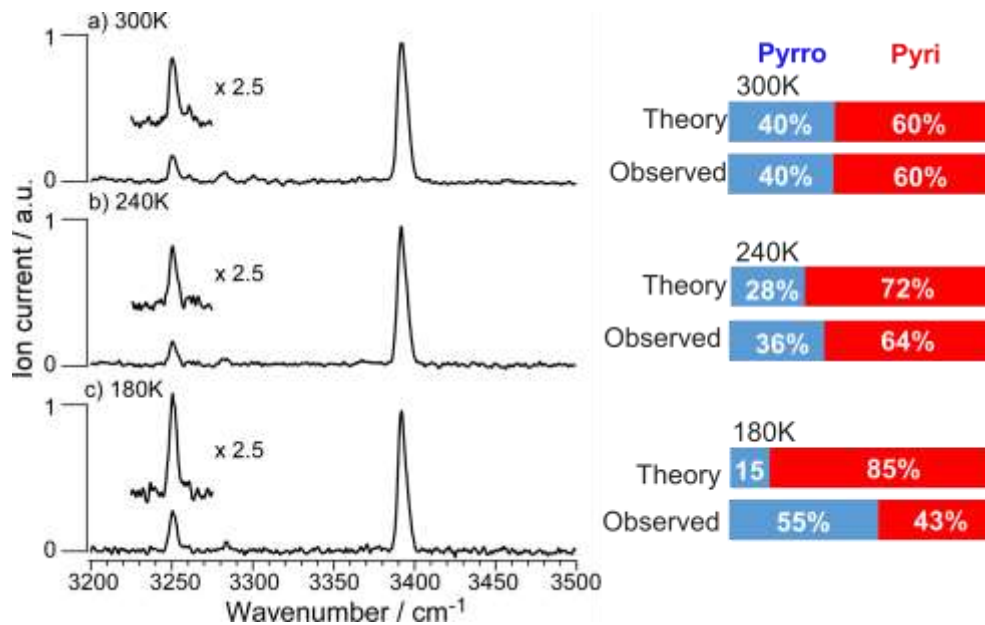


Figure 3. IRPD spectra of NIC-H⁺ with thermalizing trap filled by He gas and H₂O vapor at a) 300 K, b) 240 K, and c) 180 K. Relative intensities of NH stretching bands of two protomers changes with temperature. Observed and calculated relative populations of Pyrro-NIC-H⁺ and Pyri-NIC-H⁺ are shown besides each spectrum.

change. This finding shows the catalytic role of water in achieving the equilibrium between the two protomers.

We calculated the relative population $P_{i,exp}$ between Pyrro-NIC-H⁺ and Pyri-NIC-H⁺ using the experimental band intensity (I_{exp}) and the calculated absorption cross section (I_{calc})

$$P_{i,exp} \propto \frac{I_{exp}}{I_{calc}} \quad (2)$$

We also estimated the relative population from theoretical results ($P_{i,calc}$) of Pyri-NIC-H⁺ and Pyrro-NIC-H⁺ by Eq. (1) using the calculated ΔG_i values (see S4, S6-S9 in the SI). The estimated populations of Pyrro-NIC-H⁺ and Pyri-NIC-H⁺ at 180 K, 240 K and 300 K via Eq. (2) are shown in Figure 3. Theoretically, Pyri-NIC-H⁺ becomes dominant at lower temperatures, from 60% at 300 K up to 85% at 180 K. This temperature effect is caused by the entropic difference between protomers. The observed relative population at 300 K is Pyrro-NIC-H⁺ : Pyri-NIC-H⁺ = 40:60, which is coincidentally exactly the same as the theoretical prediction. The observed population of Pyri-NIC-H⁺ at 240 K increases up to 64%; it is essentially the same as the theoretical prediction and supports the entropic effect that makes Pyri-NIC-H⁺ dominant at lower temperatures. Interestingly, the population of Pyri-NIC-H⁺ decreases down to 43% at 180 K. This discontinuous population change is also observed in the temperature dependence of GYG-M⁺ (M : alkaline metals) complexes, and rationalized by kinetic trapping in the thermalizing trap.²⁴ If the barrier of proton transfer between pyrrolidine and pyridine sites is sufficiently high, the equilibrium between the protomers cannot be achieved at lower temperatures because of insufficient thermal energy even with the presence of the catalytic water molecules. Indeed, the observed population ratio at 180 K is Pyrro-NIC-H⁺ : Pyri-NIC-H⁺ = 55:45, which is the same ratio observed without the thermalizing trap. Since the measurement without the thermalizing trap is suspect to kinetic trapping, this finding supports that kinetic trapping is present in the low-temperature thermalizing trap. On the other hand, the experiment and theoretical population ratios coincide at 300 K, and thus we can expect that the kinetic trapping in the thermalizing trap does not take place at this temperature. From these results, we can conclude that 1) NIC-

H⁺ in the gas phase at room temperature is a mixture of Pyrro-NIC-H⁺ and Pyri-NIC-H⁺, and 2) the population ratio is 2:3 (Pyrro-NIC-H⁺ : Pyri-NIC-H⁺) at 300 K, i.e. Pyri-NIC-H⁺ is the major component. These conclusions are in sharp contrast to the previous reports suggesting the dominance of Pyri-NIC-H⁺ based on IRMPD spectroscopy in the mid-IR range and a Pyrro-NIC-H⁺ dominant mixture (pyrrolidine : pyridine = 2:1) obtained by FT-ICR-MS.¹¹

We also measured the IRPD spectrum of NOR-H⁺ that is shown in Figure 4c. In the N-H stretching region, a strong band at 3394 cm⁻¹ and three weak bands at 3276, 3322 and 3408 cm⁻¹ are observed. Our previous calculations¹⁵ predict the existence of a single Pyri-NOR-H⁺ (S, *trans*, *anti*) protomer because of the much higher energy (> 5 kcal/mol) of Pyrro-NOR-H⁺ protomers. The theoretical spectra of the Pyri-NOR-H⁺ and the Pyrro-NOR-H⁺, calculated at the same level as NIC-H⁺, are shown in Figure 4a and 4b, respectively. The theoretical spectra of Pyri-NOR-H⁺ (Figure 3b) shows the pyridine and the pyrrolidine N-H stretches at 3393 cm⁻¹ (145 km mol⁻¹) and 3408 cm⁻¹ (19 km mol⁻¹), respectively. These bands coincide the experimentally observed strong and weak bands at 3394 and 3408 cm⁻¹. The theoretical spectrum of Pyrro-NOR-H⁺ (Figure 4b) predicts the pyrrolidine anti-symmetric- and symmetric-NH₂ stretches at 3342 cm⁻¹ (70 km mol⁻¹) and 3282 cm⁻¹ (45 km mol⁻¹), respectively. From the theoretical calculations, the observed bands at 3276 and 3322 cm⁻¹ are assigned to the symmetric and anti-symmetric NH₂ stretches of Pyrro-NOR-H⁺. However, such a clear appearance of Pyrro-NOR-H⁺ is not consistent with the theoretical prediction that Pyri-NOR-H⁺ 100% dominates the population even at 300 K. Thus, the observation of Pyrro-NOR-H⁺ indicates that the dominant protomer in solution (Pyrro-NOR-H⁺) remained in the gas phase through kinetic trapping.

To avoid kinetic trapping, we introduced water vapor into the thermalizing trap with He buffer gas and repeated the measurements. Figure 5 shows the IRPD spectra of NOR-H⁺ under the presence of catalytic water molecules at (a) 300K, (b) 240 K and (c) 180K. Clearly, the vibrational signature of Pyrro-NOR-H⁺ becomes very weak at all temperatures. Even by thermalization at 300 K (Figure 5a), the population of Pyrro-NOR-H⁺ is only 8%, and decreases to 5% at 240 K, and 0% at 180 K. It strongly indicates that the kinetically trapped species are efficiently annealed by the thermalizing trap with the catalytic water molecules. The observed results are essentially consistent with the theoretical prediction that the Pyri-NOR-H⁺ is the dominant protomer (see Figure 5). We therefore conclude that NOR-H⁺ at room temperature mostly (over 90%) consists of the Pyri-NOR-H⁺ protomer. This temperature effect on NOR-H⁺ also supports the interpretation of populations in NIC-H⁺ discussed above.

4. Conclusions and Outlook

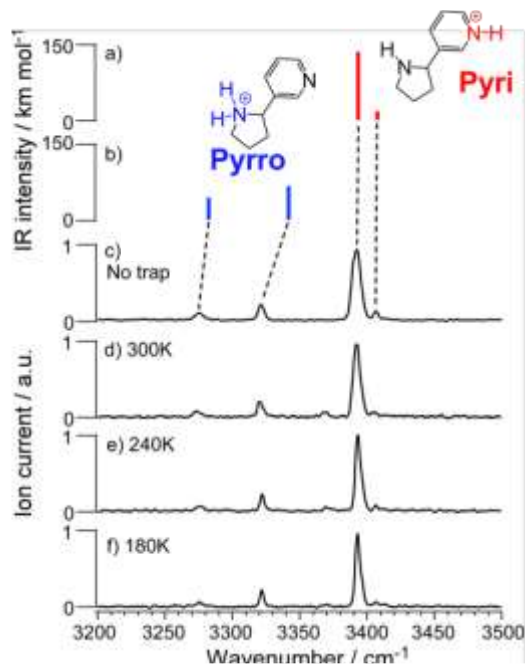


Figure 4. Theoretical IR spectra of (a) Pyri-NOR-H⁺ and (b) Pyrro-NOR-H⁺ in the 3200–3500 cm⁻¹ spectral range. The theoretical spectra were calculated at the ω B97XD/aug-cc-pVTZ level (scaling factor: 0.941). Experimental IRPD spectra of NOR-H⁺ c) without thermalizing trap, with thermalizing trap at d) 300 K, e) 240 K and f) 180 K of He buffer gas only. No change in relative intensity between Pyrro- and Pyri-NOR-H⁺ are found.

The finding that gas phase NIC-H⁺ consists of both pyrrolidine- and pyridine-protomers with populations 2:3, not only unequivocally resolves the long-lasting issue of the gas phase protonation sites, but also has significant implications for the biological role of NIC in nAChRs. Although the positions of the hydrogen atoms cannot be resolved via X-ray diffraction measurements, it is assumed that NIC is protonated on the pyrrolidine nitrogen in the nAChRs.⁶

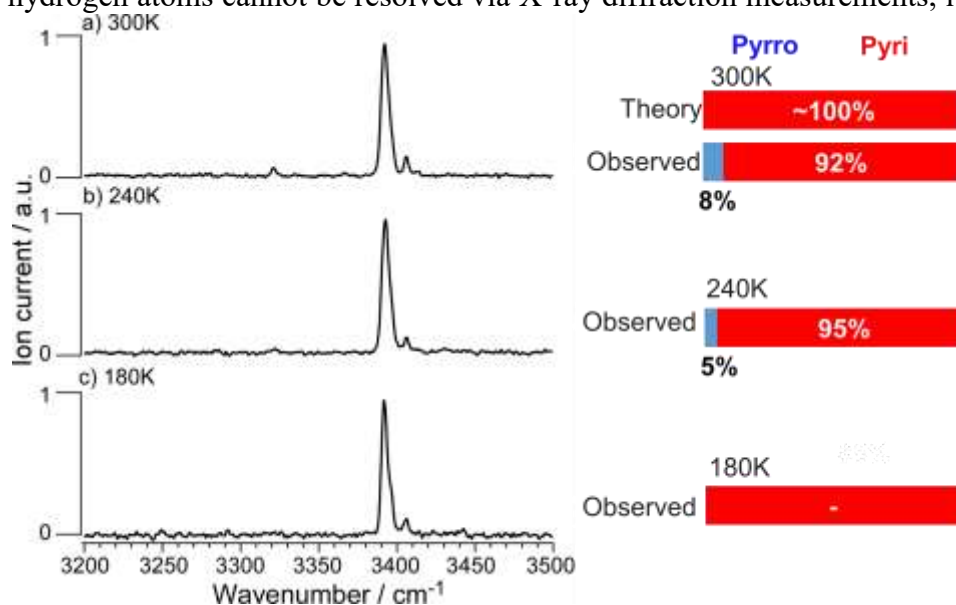


Figure 5. (a)-(c) IRPD spectra of NIC-H⁺ with the thermalizing trap filled with He gas and H₂O vapor. The temperature of the thermalizing trap is indicated in the figure. Relative intensities of NH stretching bands of two protomers changes by temperature change. Observed and calculated relative populations of Pyrro-NIC-H⁺ and Pyri-NIC-H⁺ at 180 K, 240 K and 300 K are shown beside each spectrum.

This is because the distance between the carbonyl oxygen in Trp and the pyrrolidine nitrogen is close enough (~3.1 Å) to form a hydrogen bond.⁶ The relative stability of the NIC protomers in the gas phase has been established via our joint experimental and theoretical approach. Probably the most important finding for the protonation site in the receptor is that the relative energy between the Pyrro- and Pyri-NIC protomers are reasonably close and thus their population can be easily affected by the environment, in particular the one in the binding pocket, where, besides steric interactions, there are additional cation – π and cation – dipole interactions.

These may effectively alter the gas phase energy ordering of the protomers. In contrast, the energy gap between the various NOR protomers is larger, a fact that makes the change in conformation from the aqueous phase to the pocket more difficult for NOR. Since Pyrro-NIC-H⁺ is accessible in the gas phase, it is likely also accessible in the hydrophobic pocket of the nAChR. Indeed, the Pyrro-NIC-H⁺ protomer (N, *trans*, *anti*) that we observed has the closest conformational resemblance (RMSD=0.271, see Figure S10 in SI) with the X-ray structure of nicotine in the nicotinic acetylcholine receptor (nAChR). In contrast, NOR does not have an accessible pyrrolidine-protomer and thus is less accessible in the hydrophobic pocket, leading to the decrease in addictiveness. In any sense, the precise and reliable determination of relative protomer populations of NIC-H⁺ is fundamental in interpreting the recognition mechanism of NIC-H⁺ in the receptor and will can provide valuable information for drug-design targeting the nAChRs.

Previous theoretical calculations have reported that the pyrrolidine protomer is stable when nicotine is hydrated with four molecules of water.⁴² The effect of hydration by such a small number of water molecules on the stability of protomers is currently being investigated using gas-phase molecular clusters and will be reported in the near future.

ASSOCIATED CONTENT

Supporting Information

Experimental setup, optimized geometries of NIC and NOR protomers, thermodynamic data and comparison of gas phase protomers to X-ray structure (PDF).

AUTHOR INFORMATION

Corresponding Author

* Masaaki Fujii (mfujii@res.titech.ac.jp), Shun-ichi Ishiuchi (ishiuchi.s.aa@m.titech.ac.jp), Sotiris S. Xantheas (sotiris.xantheas@pnnl.gov, xantheas@uw.edu)

Author Contributions

S. S. X., S. I., and M. F. designed the project. N. T., K. H., K. T., and S. I. conducted experiment, whereas G. S. and S. X. performed calculations. The manuscript was written through contributions of all authors. All authors have given approval to the final version of the manuscript.

Funding Sources

KAKENHI (JP18H01938, JP19H05527, JP19K23624, JP20H00372) and the Core-to-core program (JPJSCCA20210004) of JSPS, World Research Hub Initiatives in Tokyo Institute of Technology, the Cooperative Research Program of the “Network Joint Research Center for Materials and Devices” from the Ministry of Education, Culture, Sports, Science and Technology (MEXT), Japan, and the RIKEN Pioneering Project, “Fundamental Principles Underlying the Hierarchy of Matter: A Comprehensive Experimental Study”. SSX acknowledges support from the US Department of Energy, Office of Science, Office of Basic Energy Sciences, Division of Chemical Sciences, Geosciences and Biosciences at Pacific Northwest National Laboratory (PNNL). PNNL is a multiprogram national laboratory operated for DOE by Battelle.

ACKNOWLEDGMENT

The computations were performed at the Research Center for Computational Science, Okazaki, Japan, and at the National Energy Research Scientific Computing Center, which is supported by the Office of Science of the U.S. Department of Energy under Contract No. DE-AC02-05CH11231. This work was supported in part by KAKENHI (JP18H01938, JP19H05527, JP19K23624, and JP20H00372) of JSPS, the World Research Hub Initiatives in Tokyo Institute of Technology, the Cooperative Research Program of the “Network Joint Research Center for Materials and Devices” from the Ministry of Education, Culture, Sports, Science and Technology (MEXT), Japan, and the RIKEN Pioneering Project, “Fundamental Principles Underlying the Hierarchy of Matter: a Comprehensive Experimental Study”.

ABBREVIATIONS

NIC, nicotine, NOR, nornicotine, Pyri-NIC-H⁺, pyridine-protonated nicotine, Pyrro-NIC-H⁺, pyrrolidine-protonated nicotine, Pyri-NOR-H⁺, pyridine-protonated nornicotine, Pyrro-NOR-H⁺, pyrrolidine-protonated nornicotine.

REFERENCES

- (1) Griffiths, R. R.; Bigelow, G. E.; Liebson, I. Facilitation of human tobacco self-administration by ethanol: A behavioral analysis. *J. Exp. Anal. Behav.* **1976**, *25*, 279-292.
- (2) Dani, J. A.; De Biasi, M. Cellular mechanisms of nicotine addiction. *Pharmacol. Biochem. Behav.* **2001**, *70*, 439-446.
- (3) Benowitz, N. L. Pharmacology of nicotine: Addiction, smoking-induced disease, and therapeutics. *Annu. Rev. Pharmacol. Toxicol.* **2009**, *49*, 57-71.
- (4) Holladay, M. W.; Dart, M. J.; Lynch, J. K. Neuronal nicotinic acetylcholine receptors as targets for drug discovery. *J. Med. Chem.* **1997**, *40*, 4169-4194.
- (5) Brejc, K.; van Dijk, W. J.; Klaassen, R. V.; Shuurmans, M.; van der Oost, J.; Smit, A. B.; Sixma, T. K. Crystal structure of an ACh-binding protein reveals the ligand-binding domain of nicotinic receptors. *Nature* **2001**, *411*, 269-276.
- (6) Celie, P. H. N.; van Rossum-Fikkert, S. E.; van Dijk, W. J.; Brejc, K.; Smit, A. B.; Sixma, T. K. Nicotine and carbamylcholine binding to nicotinic acetylcholine receptors as studied in AChBP crystal structures. *Neuron* **2004**, *41*, 907-914.
- (7) Unwin, N. Refined structure of the nicotinic acetylcholine receptor at 4Å resolution. *J. Mol. Biol.* **2005**, *346*, 967-989.
- (8) Morales-Perez, C. L.; Noviello, C. M.; Hibbs, R. E. X-ray structure of the human $\alpha 4\beta 2$ nicotinic receptor. *Nature* **2016**, *538*, 411-415.
- (9) Walsh, R. M., Jr.; Roh, S. H.; Gharpure, A.; Morales-Perez, C. L.; Teng, J.; Hibbs, R. E. Structural principles of distinct assemblies of the human $\alpha 4\beta 2$ nicotinic receptor. *Nature* **2018**, *557*, 261-265.
- (10) Clayton, P. M.; Vas, C. A.; Bui, T. T. T.; Drake, A. F.; McAdam, K. Spectroscopic investigations into the acid-base properties of nicotine at different temperatures. *Anal. Methods* **2013**, *5*, 81-88.

- (11) Graton, J.; Berthelot, M.; Gal, J.-F.; Girard, S.; Laurence, C.; Lebreton, J.; Le Questel, J.-Y.; Maria, P.-C.; Naus, P. Site of protonation of nicotine and nornicotine in the gas phase pyridine or pyrrolidine nitrogen. *J. Am. Chem. Soc.* **2002**, *124*, 10552-10562.
- (12) Seydou, M.; Gregoire, G.; Liquier, J.; Lemaire, J.; Schermann, J. P.; Desfrancois, C. Experimental observation of the transition between gas-phase and aqueous solution structures for acetylcholine, nicotine, and muscarine ions. *J. Am. Chem. Soc.* **2008**, *130*, 4187-4195.
- (13) Marlton, S. J. P.; McKinnon, B. I.; Ucur, B.; Maccarone, A. T.; Donald, W. A.; Blanksby, S. J.; Trevitt, A. J. Selecting and identifying gas-phase protonation isomers of nicotineH⁺ using combined laser, ion mobility and mass spectrometry techniques. *Faraday Discuss.* **2019**, *217*, 453-475.
- (14) Williams, J. P.; Nibbering, N. M.; Green, B. N.; Patel, V. J.; Scrivens, J. H. Collision-induced fragmentation pathways including odd-electron ion formation from desorption electrospray ionisation generated protonated and deprotonated drugs derived from tandem accurate mass spectrometry. *J. Mass Spectrom.* **2006**, *41*, 1277-1286.
- (15) Yoshida, T.; Farone, W. A.; Xantheas, S. S. Isomers and conformational barriers of gas-phase nicotine, nornicotine, and their protonated forms. *J. Phys. Chem. B* **2014**, *118*, 8273-8285.
- (16) Warnke, S.; Seo, J.; Boschmans, J.; Sobott, F.; Scrivens, J. H.; Bleiholder, C.; Bowers, M. T.; Gewinner, S.; Schollkopf, W.; Pagel, K., et al. Protomers of benzocaine: Solvent and permittivity dependence. *J. Am. Chem. Soc.* **2015**, *137*, 4236-4242.
- (17) Sato, E.; Hirata, K.; Lisy, J. M.; Ishiuchi, S.; Fujii, M. Rethinking ion transport by ionophores: Experimental and computational investigation of single water hydration in valinomycin-K⁺ Complexes. *J. Phys. Chem. Lett.* **2021**, *12*, 1754-1758.
- (18) Ghosheh, O. A.; Dwoskin, L. P.; Li, W.-K.; Crooks, P. A. Residence times and half-lives of nicotine metabolites in rat brain after acute peripheral administration of [2'-¹⁴C] nicotine. *Drug Metab. Dispos.* **1999**, *27*, 1448-1455.
- (19) Ghosheh, O. A.; Dwoskin, L. P.; Miller, D. K.; Crooks, P. A. Accumulation of nicotine and its metabolites in rat brain after intermittent or continuous peripheral administration of [2'-¹⁴C] nicotine. *Drug Metab. Dispos.* **2001**, *29*, 645-651.
- (20) Siminszky, B.; Gavilano, L.; Bowen, S. T.; Dewey, R. E. Conversion of nicotine to nornicotine in *Nicotiana tabacum* is mediated by CYP82E4, a cytochrome P450 monooxygenase. *Proc. Nat. Acad. Sci. USA* **2005**, *102*, 14919-14924.
- (21) Papke, R. L.; Dwoskin, L. P.; Crooks, P. A. The pharmacological activity of nicotine and nornicotine on nAChRs subtypes: Relevance to nicotine dependence and drug discovery. *J. Neurochem.* **2007**, *101*, 160-167.
- (22) Fujita, T.; Nakajima, M.; Soeda, Y.; Yamamoto, I. Physicochemical properties of biological interest and structure of nicotine and its related compounds. *Pest. Biochem. Physiol.* **1971**, *1*, 151-162.
- (23) Marsh, B. M.; Voss, J. M.; Garand, E. A dual cryogenic ion trap spectrometer for the formation and characterization of solvated ionic clusters. *J. Chem. Phys.* **2015**, *143*, 204201.
- (24) Suzuki, Y.; Hirata, K.; Lisy, J. M.; Ishiuchi, S.-i.; Fujii, M. Double Ion Trap Laser Spectroscopy of Alkali Metal Ion Complexes with a Partial Peptide of the Selectivity Filter in K⁺ Channels—Temperature Effect and Barrier for Conformational Conversions. *J. Phys. Chem. A* **2021**, doi: 10.1021/acs.jpca.1021c06440.
- (25) Stearns, J. A.; Mercier, S.; Seabey, C.; Guidi, M.; Boyarkin, O. V.; Rizzo, T. R. Conformation-specific spectroscopy and photodissociation of cold, protonated tyrosine and phenylalanine. *J. Am. Chem. Soc.* **2007**, *129*, 11814-11820.
- (26) Kamrath, M. Z.; Relph, R. A.; Guasco, T. L.; Leavitt, C. M.; Johnson, M. A. Vibrational predissociation spectroscopy of the H₂-tagged mono- and dicarboxylate anions of dodecanedioic acid. *Int. J. Mass Spectrom.* **2011**, *300*, 91-98.
- (27) Redwine, J. G.; Davis, Z. A.; Burke, N. L.; Oglesbee, R. A.; McLuckey, S. A.; Zwier, T. S. A novel ion trap based tandem mass spectrometer for the spectroscopic study of cold gas phase polyatomic ions. *Int. J. Mass Spectrom.* **2013**, *348*, 9-14.
- (28) Kang, H.; Féraud, G.; Dedonder-Lardeux, C.; Jouvét, C. New method for double-resonance spectroscopy in a cold quadrupole ion trap and its application to UV–UV hole-burning spectroscopy of protonated adenine dimer. *J. Phys. Chem. Lett.* **2014**, *5*, 2760-2764.
- (29) Garand, E. Spectroscopy of reactive complexes and solvated clusters: A bottom-up approach using cryogenic ion traps. *J. Phys. Chem. A* **2018**, *122*, 6479-6490.

- (30) Eun, H. J.; Min, A.; Jeon, C. W.; Yoo, I. T.; Heo, J.; Kim, N. J. Chiral and isomeric discrimination of chiral molecular ions by cold ion circular dichroism spectroscopy. *J. Phys. Chem. Lett.* **2020**, *11*, 4367-4371.
- (31) Ishiuchi, S.; Wako, H.; Kato, D.; Fujii, M. High-cooling-efficiency cryogenic quadrupole ion trap and UV-UV hole burning spectroscopy of protonated tyrosine. *J. Mol. Spectrosc.* **2017**, *332*, 45-51.
- (32) Otsuka, R.; Hirata, K.; Sasaki, Y.; Lisy, J. M.; Ishiuchi, S.; Fujii, M. Alkali and alkaline earth metal ions complexes with a partial peptide of the selectivity filter in K⁺ channels studied by a cold ion trap infrared spectroscopy. *ChemPhysChem* **2020**, *21*, 712-724.
- (33) Reavill, C.; Jenner, P.; Kumar, R.; Stolerman, I. P. High affinity binding of [³H] (-)-nicotine to rat brain membranes and its inhibition by analogues of nicotine. *Neuropharmacology* **1988**, *27*, 235-241.
- (34) Kisaki, T.; Tamaki, E. Phytochemical studies on tobacco alkaloids. I. Optical rotatory power of nornicotine. *Arch. Biochem. Biophys.* **1961**, *92*, 351-355.
- (35) Xantheas, S. S. On the importance of the fragment relaxation energy terms in the estimation of the basis set superposition error correction to the intermolecular interaction energy. *J. Chem. Phys.* **1996**, *104*, 8821-8824.
- (36) Bunge, C. F. Electronic wave functions for atoms. *Theo. Chim. Acta* **1970**, *16*, 126-144.
- (37) Termath, V.; Klopper, W.; Kutzelnigg, W. Wave functions with terms linear in the interelectronic coordinates to take care of the correlation cusp. II. Second-order Möller-Plesset (MP2-R12) calculations on closed-shell atoms. *J. Chem. Phys.* **1991**, *94*, 2002-2019.
- (38) Kendall, R. A.; Dunning, T. H.; Harrison, R. J. Electron affinities of the first - row atoms revisited. Systematic basis sets and wave functions. *J. Chem. Phys.* **1992**, *96*, 6796-6806.
- (39) Aprà, E.; Bylaska, E. J.; de Jong, W. A.; Govind, N.; Kowalski, K.; Straatsma, T. P.; Valiev, M.; van Dam, H. J. J.; Alexeev, Y.; Anchell, J., et al. NWChem: Past, present, and future. *J. Chem. Phys.* **2020**, *152*, 184102.
- (40) Voss, J. M.; Marsh, B. M.; Zhou, J.; Garand, E. Interaction between ionic liquid cation and water: infrared predissociation study of [bmim]⁺·(H₂O)_n clusters. *Phys. Chem. Chem. Phys.* **2016**, *18*, 18905-18913.
- (41) Jolly, W. L. *Modern Inorganic Chemistry* (2nd ed.). McGraw-Hill, New York. **1991**.
- (42) Gaigeot, M. P.; Cimas, A.; Seydou, M.; Kim, J. Y.; Lee, S.; Schermann, J. P. Proton transfer from the inactive gas-phase nicotine structure to the bioactive aqueous-phase structure. *J. Am. Chem. Soc.* **2010**, *132*, 18067-18077.